

68%), mp 65–80°, which resisted crystallization. The material displayed appropriate ir and nmr spectra and tlc behavior.

t-Butyloxycarbonyl-L-prolyl-L-prolyl-L-prolyl-L-prolyl-L-prolyl Benzyl Ester (*t*-Boc-Pro₅-OBz) (XI). *t*-Boc-Pro₅-OH (3.69 g) was treated with N-methylmorpholine (1.33 ml) and isobutyl chloroformate (1.62 ml) as described above. After formation of the mixed anhydride, HCl·H-Pro₅-OBz (6.30 g, prepared by subjecting 7.0 g of *t*-Boc-Pro₅-OBz to the action of HCl-ethyl acetate for 1 hr as indicated above) and N-methylmorpholine (1.33 ml) were successively added and the mixture was stirred overnight. Work-up as described above gave *t*-Boc-Pro₅-OBz (XI) as a yellowish syrup (9.2 g, 94%), which when dissolved in a small amount of ethyl acetate gave, on standing, crystalline *t*-Boc-Pro₅-OBz (first crop 1.0 g), mp 221–229°. The material displayed appropriate ir and nmr spectra and tlc behavior.

Anal. Calcd for C₄₂H₅₈N₆O₉·H₂O: C, 62.35; H, 7.47; N, 10.39. Found: C, 62.45; H, 7.44; N, 10.29.

In another run, *t*-Boc-Pro₅-OH (1.0 g) was treated with N-methylmorpholine (0.28 ml) and isobutyl chloroformate (0.29 ml) as described. After mixed anhydride formation, HCl·H-Pro₅-OBz (1.07 g) and N-methylmorpholine (0.28 ml) were added. Overnight stirring and work-up as usual gave crude *t*-Boc-Pro₅-OBz (1.0 g, 60%), which when crystallized from ethyl acetate gave a first crop of crystalline material (0.36 g), mp 221–224°, which was identical with the "2 + 4" *t*-Boc-Pro₅-OBz.

t-Butyloxycarbonyl-L-prolyl-L-prolyl-L-prolyl-L-prolyl-L-prolyl-L-proline (*t*-Boc-Pro₅-OH) (XII). *t*-Boc-Pro₅-OBz (0.9 g) was dissolved in 15 ml of *t*-butyl alcohol, treated with 10% Pd/C, and subjected to the hydrogenation conditions described above. Filtration of catalyst and solvent removal gave 0.8 g (100%) of an amorphous foam which dissolved slowly in boiling ethyl acetate, and yielded, on standing, crystals of *t*-Boc-Pro₅-OH (XII) (first crop 0.46 g) which had mp 229–231°, and displayed ir and nmr spectra and tlc behavior appropriate for the expected compound.

Anal. Calcd for C₃₅H₅₂N₆O₅: C, 59.98; H, 7.48; N, 11.99. Found: C, 59.71; H, 7.75; N, 11.70.

t-Butyloxycarbonylglycyl-L-prolyl Benzyl Ester (*t*-Boc-Gly-L-Pro-OBz) (XIII). *t*-Butyloxycarbonylglycine (19.6 g) was dissolved in 270 ml of chloroform and cooled to –20° in a Dry Ice-CCl₄ cooling bath. Triethylamine (15.5 ml) and isobutyl chloroformate (14.4 ml) were added with stirring. After 30 min, L-proline benzyl ester hydrochloride (26.7 g) was added, followed by an additional equivalent of triethylamine (15.5 ml). After over-

night stirring, work-up was accomplished by extractions of the reaction mixture successively with 200-ml portions of water, 5% aqueous sodium bicarbonate, and saturated sodium chloride. The chloroform layer was dried over sodium sulfate and evaporated to give a colorless syrup (41.0 g, 100%). When 10 g of this syrup was dissolved in a minimum of ethyl acetate and hexane was added to the cloud point, shiny crystals of *t*-Boc-Gly-L-Pro-OBz (XIII) formed (first crop 5.4 g). The crystals had mp 76–77°, and showed appropriate ir and nmr spectra and tlc behavior.

Anal. Calcd for C₁₆H₂₆N₂O₅: C, 62.96; H, 7.23; N, 7.73. Found: C, 62.96; H, 7.14; N, 7.71.

t-Butyloxycarbonylglycyl-L-proline (*t*-Boc-Gly-L-Pro-OH) (XIV). A solution of *t*-Boc-Gly-L-Pro-OBz (30 g) in 150 ml of *t*-butyl alcohol was treated with a catalytic amount of 10% Pd/C and hydrogenated at 20 psi for 30 hr at room temperature. Filtration through a pad of Celite to remove the catalyst followed by evaporation of the solvent gave a syrup. Crystallization from ethyl acetate-ether gave *t*-Boc-Gly-L-Pro-OH (XIV), first crop 10.0 g (45%), mp 126–135°, ir and nmr spectra and tlc behavior appropriate for the expected compound. A small amount of material which was crystallized in a similar fashion for analytical data had the same melting point.

Anal. Calcd for C₁₂H₂₀N₂O₅: C, 52.8; H, 7.4; N, 10.2. Found: C, 53.1; H, 7.6; N, 10.2.

Poly-L-proline. The sample of this polymer employed for these studies was prepared according to the method of Fasman and Blout.⁵ The anhydride-initiator (sodium methoxide) ratio was 10, and the acetonitrile-insoluble fraction of the polymer was used. The reduced specific viscosity of this sample, determined on a solution of 15.0 mg of polymer in 10 ml of dichloroacetic acid, was 0.0296. From these data, the molecular weight of the sample, while not determined directly, was less than 5000. Higher polymers of proline were not sufficiently soluble in chloroform to allow nmr studies.

Acknowledgment. We are pleased to acknowledge support in part of this work by U.S. Public Health Service Grants No. AM-07300 and AM-10794. One of us (C. M. D.) held a Public Health Service Postdoctoral Fellowship (No. AM-20628) in the years 1967–1969. We thank Mr. J. J. Ryan and Mrs. A. I. Brewster for expert technical assistance in recording nmr spectra.

The Organic Solid State. III. Spectroscopic and Electrical Properties of Biferrocene[Fe(II)Fe(III)] Picrate¹

F. Kaufman² and D. O. Cowan³

Contribution from the Department of Chemistry, The Johns Hopkins University, Baltimore, Maryland 21218. Received May 4, 1970

Abstract: The mixed valence compound biferrocene[Fe(II)Fe(III)] picrate (**1**) was prepared by the benzoquinone oxidation of biferrocene in the presence of picric acid. The ultraviolet, visible, and near-infrared spectra of **1** indicate transitions characteristic of the picrate anion, of ferrocene, and of ferrocenium ion. In addition a new mixed valence transition is observed (solution and solid) in the near-infrared [1900 m μ (ϵ 551)]. This new transition is discussed along with the observed shifts in metal-ligand stretching frequencies (far-infrared) which are known to be strongly dependent on the oxidation state of the central iron atom. This mixed valence compound was found to be six orders of magnitude more conducting than either ferrocene or ferrocenium picrate [$\sigma(298) = 2.3 \times 10^{-8}$ ohm⁻¹ cm⁻¹].

There are a large number of inorganic compounds which contain metal ions of the same element in two different oxidation states.⁴ Many of these mixed

valence compounds have physical properties that are strikingly different from the materials containing just one of the oxidation states. For example, Fe₂O₃ and Fe₃O₄ have almost identical iron-iron distances (3 Å)

(1) (a) The Organic Solid State. Part II: D. O. Cowan and F. Kaufman, submitted for publication. (b) Part I: D. O. Cowan and F. Kaufman, *J. Amer. Chem. Soc.*, **92**, 219 (1970).

(2) National Institutes of Health Predoctoral Fellow.

(3) A. P. Sloan Fellow; to whom correspondence should be addressed

(4) (a) M. B. Robin and P. Day, *Advan. Inorg. Chem. Radiochem.*, **10**, 247 (1967); (b) G. C. Allen and N. S. Hush, *Progr. Inorg. Chem.*, **8**, 357 (1967).

but the conductivity of Fe_3O_4 , a mixed valence Fe(II),-Fe(III) compound, is six orders of magnitude higher than Fe_2O_3 . The unusually high conductivity [2.5×10^2 (ohm cm) $^{-1}$] of Fe_3O_4 has been attributed to rapid valence oscillation between the iron sites in the material.⁵

Theory and experiment suggest that the extent of electron delocalization between the mixed valence species is of fundamental importance in determining physical properties. Unfortunately, the ligands usually used in these materials are not readily susceptible to structural variation. However, organometallic compounds offer a unique structural framework on which to orient and position the mixed valence metal atoms, and to control the extent of interaction of the metal centers. It has been shown^{4a} that strong interaction between the mixed valence centers is expected when the orbitals in question have the same symmetry and are close enough to overlap appreciably. In addition, delocalization can be further promoted when the ligand field strength or symmetry of the different ions is very similar. In light of these factors, the metallocenes were chosen as the first candidates in our study of energy transfer in mixed valence organometallic compounds.

Ferrocene is the best known member in this series of organometallic compounds. Since its discovery in 1951, a large number of monomer⁶ and polymer⁷ derivatives have been synthesized and studied. Ferrocene, with the iron formally in the 2+ oxidation state, is easily oxidized by a variety of reagents to the 3+ state, forming stable ferrocenium salts. Crystallographic data on ferrocene⁶ and its salts^{8,9} indicate that the oxidation state and charge of the iron atom have almost no effect on the interatomic distances. Therefore, little reorganizational energy is needed to make the mixed valence sites identical, and as a result it would be expected that properly oriented ferrocene and ferrocenium molecules will undergo electron exchange quite readily. This is indeed what has been experimentally observed in solution.¹⁰ Finally, the metallocenes were chosen because the strong interaction between the metal orbitals and unsaturated π system of the rings suggested that compounds might be found where mixed valence delocalization could be induced *via* metal-ligand overlap without requiring direct metal-metal interaction.

The range of unique molecular structures and electron interactions possible in mixed valence organometallic compounds may result in materials with physical properties (electrical, optical, and magnetic) which are quite different from those exhibited by the well-known inorganic and organic substances. In addition, some of the mixed valence organometallic compounds may serve as useful models in studying the short-range electron transfer, occurring during biological oxidation-reduction reactions, *via* the array of electron carriers located on the inner membranes of chloroplasts and mitochondria. In light of these considerations, we

would like to report in detail the synthesis and physical properties of biferrocene[Fe(II)Fe(III)] picrate (**1**), a mixed valence salt of ferrocene.¹¹ The vibrational and electronic spectra, as well as the electrical conductivity, demonstrate that significant mixed valence interactions have been induced in this organometallic compound.

Experimental Section

Biferrocene, prepared by the Ullman coupling of iodoferrocene,¹² was oxidized with an excess of benzoquinone in the presence of picric acid.¹³ A typical preparation involved the addition of 0.3 g (8×10^{-4} mol) of biferrocene to 75 ml of benzene containing 0.17 g (1.5×10^{-3} mol) of benzoquinone and 0.25 g (1.1×10^{-3} mol) of picric acid. The solution was allowed to stand at room temperature for several days and the resulting flocculent precipitate was collected and washed with benzene. The crude material was recrystallized from methanol-water and dried under vacuum. The black, highly reflective, plate-like crystals were obtained in 40–50% yields and were found to be stable in air at room temperature but decomposed rapidly when heated above 200°. The solid picrate salt may decompose violently if subjected to sudden shock or high pressure.

Anal. Calcd for **1** [(C₂₀H₁₈Fe₂)⁺(C₆H₂N₃O₇)⁻]: C, 52.2; H, 3.37; Fe, 18.6. Found: C, 52.0; H, 3.47; Fe, 18.0 (calcd from ash).

Electronic spectra were obtained on a Cary 14 recording spectrophotometer. All solutions (Spectrograde acetonitrile) were degassed with prepurified nitrogen and were used immediately after they were prepared.

Infrared spectra were measured on a Perkin-Elmer Model 521 grating instrument. Samples were run as KBr pellets or as a Nujol mull on NaCl or CsBr plates.

Electrical Measurements. The electrical conductivity was determined by applying a constant dc potential, from a Keithley 241 regulated power supply, along the long axis of a crystal of **1**. The resulting current through the crystal was measured with a Keithley 602 electrometer.

A single crystal was mounted on a quartz wafer and electrical contact to 0.003-in. Cu leads was made with du Pont silver preparation No. 4817 or Allied Products Corp. No. 3027 conductive epoxy. (The size of the crystals precluded the use of four electrodes or a guard ring.)

All measurements were performed in a shielded sample holder to guard against stray external fields. The conductivity was measured for a number of crystals from different preparations in a nitrogen atmosphere; in addition, the conductivity was measured in both voltage directions (polarity reversed).

Results and Discussion

Infrared Spectroscopy. The ir spectrum of **1**, in the region 4000–500 cm^{-1} , shows absorptions due to the biferrocenyl and picrate portions of the salt. The following nonpicrate transitions have been assigned by a comparison with ferrocene,¹⁴ biferrocene,¹⁵ and ferrocenium picrate:¹⁶ ir (Nujol mull) 3085 (C–H stretch); 1414 (C–C antisymmetric stretch); 1109, 1102 (antisymmetric ring breathing); 1002 (C–H bend ||); 812 cm^{-1} (C–H bend \perp).

In the far-infrared, there are nonpicrate absorptions at 489, 445, and 399 cm^{-1} (KBr pellet and Nujol mull). To understand the absorptions in this region of the spectrum, it is necessary to discuss the band assignments for the unsubstituted species. Ferrocene⁶ has an antisymmetric ring-tilt transition at 492 cm^{-1} and an anti-

(5) A. Rosencwaig, *Can. J. Phys.*, **47**, 2309 (1969).

(6) M. Rosenblum, "Chemistry of the Iron Group Metallocenes," New York, N. Y., 1965.

(7) E. W. Neuse, "Advances in Macromolecular Chemistry," W. M. Pasika, Ed., Academic Press, New York, N. Y., 1968.

(8) R. C. Pettersen, Ph.D. Thesis, The University of California, Berkeley, Calif., 1966.

(9) T. Bernstein and F. H. Herbstein, *Acta Crystallogr.*, *Sect. B*, **24**, 1640 (1968).

(10) D. R. Stranks, *Discuss. Faraday Soc.*, **29**, 73 (1960).

(11) For a preliminary account *cf.* ref 1b.

(12) M. D. Rausch, *J. Org. Chem.*, **6**, 1802 (1961).

(13) G. Wilkinson, M. Rosenblum, M. C. Whiting, and R. B. Woodward, *J. Amer. Chem. Soc.*, **74**, 2125 (1952); L. M. Epstein, *J. Chem. Phys.*, **36**, 2731 (1962).

(14) E. R. Lippincott and R. O. Nelson, *Spectrochim. Acta*, **10**, 307 (1958); D. Hartley and M. J. Ware, *J. Chem. Soc. A*, 138 (1969).

(15) Unpublished data of F. Kaufman.

(16) I. Pavlik and J. Klikorka, *Collect. Czech. Chem. Commun.*, **30**, 664 (1965).

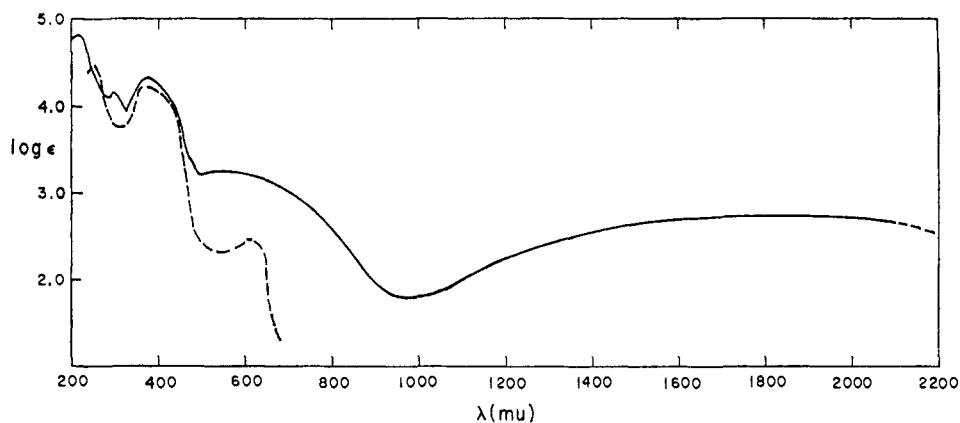


Figure 1. Visible-ultraviolet near-infrared spectra of biferrrocene[Fe(II)Fe(III)] picrate (**1**), solid line; spectra of ferrocene(III) picrate, broken line.

symmetric metal-ligand stretching transition at 478 cm^{-1} . Oxidation of the central iron atom to the 3+ state, giving the ferrocenium ion, is reported¹⁶ to lower the frequency of the latter transition to $405\text{--}423\text{ cm}^{-1}$. This spectral shift is due to weakened bonding between the central iron atom and cyclopentadienyl rings in the ferrocenium cation.¹⁶ A similar decrease in stretching frequency is found on going from ferrocyanide to ferricyanide ($\Delta = 79\text{ cm}^{-1}$). Because the iron-ligand bond strength seems to be strongly dependent on the electronic configuration of the metal atom, the iron-ligand antisymmetric stretching transition can be used to determine the oxidation state of the iron in ferrocene compounds. In the case of **1**, a binuclear mixed valence ferrocene salt, the number and position of these transitions may help to describe the extent of metal-metal interaction and the actual metal valence state(s) of the compound.

It is tempting to assign the 489-cm^{-1} absorption to antisymmetric ring-tilt transitions of the cyclopentadienyl rings. The 445- and 399-cm^{-1} absorptions can then be assigned as the metal-ligand stretching transitions of the ferrocene and ferrocenium portions of **1**, respectively. This is consistent with the elemental analysis data which indicate that only one iron atom in the molecule has been oxidized (monopicrate formed). The shifts to longer wavelength of these transitions can be interpreted to mean that the two halves of the molecule are not isolated but interact in some manner which is not readily apparent from this information alone. Further data on the way in which donor and acceptor groups affect the metal-ligand stretching frequencies in ferrocene compounds are needed to substantiate these tentative band assignments.

Electronic Spectroscopy. The electronic spectrum of **1**, from 200 to 2000 $\text{m}\mu$, is shown in Figure 1. There are at least five transitions observed in this wavelength region. The band at $375\text{ m}\mu$ in both ferrocenium picrate and **1** is assigned to a transition of the picrate anion (picrate anion in acetonitrile, $\lambda_{\text{max}} 358 \pm 15\text{ m}\mu$ depending on the counterion). The bands at 220 and $295\text{ m}\mu$ are due to transitions of the substituted ferrocene portion of **1** in analogy to the bands observed for biferrrocene [$\text{uv max (EtOH) } 220 (\epsilon 4.70 \times 10^4)$, $295 (\epsilon 8.57 \times 10^3)$, $450\text{ m}\mu (\epsilon 649)$]. The band at $450\text{ m}\mu (\epsilon 91)$ in ferrocene is probably obscured by picrate absorption in the spectrum of **1**.

Neither ferrocene nor biferrrocene has transitions at wavelengths longer than $450\text{ m}\mu$ but ferrocenium picrate has a band at $617\text{ m}\mu (\epsilon 340)$. This band has been assigned as the ${}^2E_{2g}[(a_{1g})^2(e_{2g})^3]$ to ${}^2A_{1g}[(a_{1g})^4(e_{2g})^4]$ transition of the ferrocenium ion by Scott and Becker.¹⁷ In analogy to this band, the broad band in the spectrum of **1** centered at $550\text{--}600\text{ m}\mu (\epsilon 1860)$, acetonitrile is assigned to the substituted ferrocenium portion of **1**. The visible region of the electronic spectrum in Figure 1 indicates the striking comparison between the ferrocene ion band in the unsubstituted parent and in biferrrocene[Fe(II)Fe(III)] picrate. The mixed valence salt has a transition which is broader, is three times more intense, and is shifted to shorter wavelengths, in comparison with the ferrocenium picrate transition. These factors indicate that the two ferrocene chromophores are not isolated and that there exists some intramolecular interaction between the ferrocenium chromophore and the adjacent ferrocene substituent. Though the effect of conjugation between the cyclopentadienyl rings in biferrrocene has been noted¹⁸ in the literature, this is the first account of spectral properties and intramolecular interaction in a biferrrocene compound in which the two metal atoms exist in different valence states.

The presence of the band at $550\text{--}600\text{ m}\mu$ is not consistent with the formulation of compound **1 as a molecular (π) complex of picric acid and biferrrocene.** Other evidence that favors the structure proposed rather than a molecular complex includes: (a) thermal stability of **1**; (b) all bands in the spectra of **1** obey Beer's law and are independent of added picric acid, with the exception of the $375\text{-m}\mu$ picrate band; (c) the spectral band positions of **1** are observed to be independent of solvent polarity; (d) compound **1** possesses ir bands not present in either biferrrocene or picric acid; and (e) compound **1** is not formed in the absence of an oxidizing agent.

In the near-ir region of the spectrum a new band (mixed valence band) is observed at $1900\text{ m}\mu (\epsilon 551)$. This absorption could be due to an electron-transfer transition¹¹ whereby optical excitation provides the energy necessary for electron exchange between the

(17) (a) D. R. Scott and R. S. Becker, *J. Phys. Chem.*, **69**, 3207 (1965); *J. Chem. Phys.*, **35**, 516 (1961); A. T. Armstrong, F. Smith, E. Elder, and S. P. McGlynn, *ibid.*, **46**, 4321 (1967); A. T. Armstrong, D. G. Carroll, and S. P. McGlynn, *ibid.*, **47**, 1104 (1967). (b) For a more recent interpretation see R. Prins, *Chem. Commun.*, 284 (1970).

(18) S. I. Goldberg, D. W. Mayo, and J. A. Alford, *J. Org. Chem.*, **28**, 1708 (1963).

mixed valence iron atoms (Figure 2). It would not be reasonable to assign the 1900-m μ band as an overtone of a vibrational mode based on the transition half-width (5000 cm⁻¹), intensity, or position relative to known ir and Raman bands.

At least in part, the width of this and other electron-transfer bands may be explained by observing that the equilibrium distance between the two metal centers (reactant and product) can vary somewhat from molecule to molecule. This gives rise to a large number of allowed Franck-Condon transitions¹⁹ (see Figure 2). The assignment of the 1900-m μ band to an electron-transfer transition is consistent with Taube's assignment of the 1570-m μ band in a mixed valence ruthenium complex²⁰ to an electron-transfer transition. The Ru(II)-Ru(III) distance in Taube's relatively rigid complex is about 6.8 Å while the Fe(II)-Fe(III) distance in **1** has been calculated from models to be from 3.8 (cis coplanar) to 5.1 Å (trans coplanar). If the half-width ($\Delta\bar{\nu}_{1/2}$) of the electron-transfer band does depend on the range of distances between the two metal centers then compound **1** should exhibit a broader band than the rigid ruthenium complex. The half-width of the 1900-m μ band of **1** is three times as broad as the corresponding 1570-m μ band of the ruthenium complex (see Table I). Table I also gives the predicted

Table I. Observed and Calculated Electron-Transfer Transition-Band Half-Widths

Compd	ν_{\max} , cm ⁻¹ (m μ)	$\Delta\bar{\nu}_{1/2}$ (calcd), ^a cm ⁻¹	$\Delta\bar{\nu}_{1/2}$ (obsd), ^b cm ⁻¹
$[(\text{NH}_3)_2\text{Ru}(\text{C}_6\text{H}_5)_2\text{NRu}(\text{NH}_3)_2]^{3+}$	6369 (1570)	3800	1600 ^c
1	5263 (1900)	3490	5000

^a $\Delta\bar{\nu}_{1/2} = 48 (\bar{\nu}_{\max})^{1/2}$. ^b Because of the band width $\Delta\bar{\nu}_{1/2}$ values are only approximate. ^c Calculated from Taube's published spectra.

half-widths for these transitions calculated on the basis of Hush's theoretical model.²¹

In this interpretation, the energy associated with the long-wavelength transition [$E_{op} = hc\bar{\nu}_{\max}$, 15.1 kcal (0.66 eV)] causes an intramolecular electron-transfer reaction by optically exciting an electron, localized on an Fe(II) atom, into a higher excited state where that electron is effectively delocalized over both metal atoms in the molecule (Figure 2). In addition, there is a thermally activated path for internal electron transfer: the molecule can absorb enough heat energy, E_{th} , to transform it into an activated complex which spontaneously may decay to give the electron-transfer isomer. We can derive information about this thermal process because it can be shown that the optical excitation energy, E_{op} , is four times the activation energy for the thermal process, E_{th} . This relationship was derived by Hush²¹ for several models and can easily be seen from simple geometrical arguments using harmonic oscillators

(19) This cannot be the only important factor inasmuch as Taube has recently observed that a fairly rigid mixed valence compound also gave a relatively broad band.⁹ However, it should be noted that when this band is graphed in terms of $\bar{\nu}$ (cm⁻¹) instead of λ (m μ) the band appears not to be exceptionally broad.

(20) C. Creutz and H. Taube, *J. Amer. Chem. Soc.*, **91**, 3988 (1969).

(21) N. S. Hush, *Progr. Inorg. Chem.*, **8**, 391 (1967).

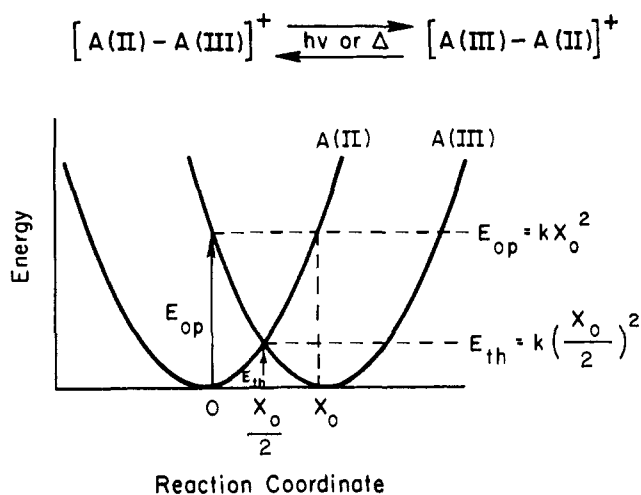


Figure 2. Potential energy-reaction coordinate diagram for a simple symmetrical one-electron transfer. The curves represent two weakly interacting states [A(II) and A(III)] at some equilibrium distance X_0 . If these states are represented as harmonic oscillators [$E(x) = k\Delta X^2$] then the maximum for the optical transition (Franck-Condon transition) is equal to kX_0^2 and the maximum for the thermal transition (at $X_0/2$) is equal to $k(X_0/2)^2$ or the thermal activation energy is one-quarter of the optical transition energy ($E_{Th} = E_{Op}/4$). If the equilibrium distance (X_0) can vary then a rather broad optical transition should be expected.

(see Figure 2). The energy barriers for the thermal intramolecular electron transfer are calculated in this manner to be $hc\bar{\nu}_{\max}/4 = 3.78$ kcal (0.16 eV). If this quantity is assumed to be equal to ΔG^\ddagger , then an intramolecular electron-transfer rate constant can be calculated ($kt/h \exp[-\Delta G^\ddagger/RT] = 1.3 \times 10^{10} \text{ sec}^{-1}$).¹⁷

A quantitative check on the reasonableness of this rate constant can be derived from the data on electron exchange between ferrocene and ferrocenium in solution. The second-order rate constant (25°) for this process can be estimated from low-temperature experimental data to be about $3.1 \times 10^8 \text{ M}^{-1} \text{ cm}^{-1}$.²² We can compare the two rate constants by calculating that a total concentration of 12 M is required to produce a solution where the average distance between ferrocene and ferrocene ion is 4.1 Å²³ (in the range of the iron-iron distance of **1**, 3.8-5 Å). This concentration, when multiplied by the bimolecular rate constant, gives a pseudo-first-order rate constant of about $4 \times 10^9 \text{ sec}^{-1}$. This value is consistent with the rate constant calculated from the near-ir transition ($1.3 \times 10^{10} \text{ sec}^{-1}$).

It is well known⁴ that inorganic mixed valence compounds show new bands, usually in the visible region, that are not seen in the spectra of either component taken alone. The mixed valence band in the organometallic compound **1** appears in the near ir and the relatively low energy of the absorption means that thermal electron transfer in this system is quite facile. Biferrocene[Fe(II)Fe(III)] picrate might be expected to show a very rapid transfer rate because the C-C bond ties two species together (in a mixed valence array) that are uniquely suited for fast exchange. Libby has proposed that because electron transfer is fast compared

(22) If the $T\Delta S^\ddagger$ term for the electron-transfer reaction is small then the free energy (ΔG^\ddagger) for this reaction is approximately equal to the activation energy (E_{th}). For the ferrocene-ferrocenium ion exchange the $T\Delta S^\ddagger$ term is less than 7% of the total free energy.¹²

(23) E. M. Kosower, "Physical Organic Chemistry," Wiley, New York, N. Y., 1968, p 344.

to nuclear motions (Franck–Condon principle), rapid electron-transfer reactions will require the initial and final states to have similar geometries and bond lengths.²⁴ The ferrocene–ferrocenium ion couple satisfies this geometrical requirement for fast exchange. Crystallographic data indicate that there is almost no change in bond lengths in going from one species to the other. The metal–ring plane distance in ferrocene⁶ is 1.63–1.66 Å while the corresponding distance in ferrocenium picrate⁹ is 1.684 ± 0.005 Å and in ferrocenium iodide⁹ is 1.65 ± 0.1 Å. In Marcus' theory for isotopic exchange reactions,²⁵ the free energy of activation is dependent on the charge of the exchanging ions and their size. In the ferrocene–ferrocenium ion case, there is exchange between a neutral and a charge species so that there are no coulombic interactions to slow the electron transfer. In the absence of these interactions this theory ascribes the activation solely to the need for reorganization of solvent molecules to form the nonequilibrium transition state. Since the solvent reorganization energy is inversely proportional to ionic radius, it can be expected that this factor is much less important for a ferrocene molecule than for the smaller, more common, inorganic iron complexes. Juxtaposition of two ferrocene molecules, as in the biferrocene skeleton, leads to a still bulkier species with a very fast, almost solvent-independent transfer rate.

Mechanisms of Intramolecular Interaction. The ferrocenium iron has a characteristic absorption peak in the visible at $617 \text{ m}\mu$.³ The mixed valence ferrocene salt **1** has a band at $560 \text{ m}\mu$, shifted almost $60 \text{ m}\mu$ from the absorption in the parent compound. This hypochromic shift may be due to the inductive influence of the ferrocene substituent or it may be due to inductive and resonance interactions between the two portions of the molecule. It is important to consider the possible mechanisms of intramolecular interaction in **1**, since this matter bears directly on the meaning of the mixed valence band and on the interpretation of other physical properties, such as the electrical conductivity.

(1) If only inductive effects are involved in the interaction of the ferrocene and ferrocenium moieties, then all electrons are localized in molecular orbitals centered around the two discrete ferrocene nuclei. One can then assign a definite integral oxidation number to each iron atom and, therefore, calculate meaningful rates of electron "hopping" from one nucleus to the other. The derivation used for the rate expression implicitly assumes negligible resonance interaction in the system so that our calculated rate of hopping, $1.3 \times 10^{10} \text{ sec}^{-1}$, applies to a molecule in which an inductive effect is the primary mechanism of intramolecular interaction. In this interpretation, the shifts in the visible band of **1** and in the metal–ligand stretching transition in the far-infrared region are ascribed to an inductive interaction with the adjacent ferrocene molecule. The inductive influence of a ferrocene substituent on the ferrocenium portion of the molecule could lead to an increase in the effective charge on the formally $2+$ iron atom, thereby decreasing the metal–ligand force constant and shifting the far-infrared transition to lower frequency. In this picture the metal–ligand stretching frequency of ferrocenium would seem to be

relatively insensitive to substituent effects. On the other hand, the ferrocenium transition in the visible region of the spectrum is quite sensitive to the adjacent ferrocene moiety. The use of a substituent which transforms the biferrocene molecule into a mixed valence species results in an increase in energy difference for the two states involved in the spectral transition. This net destabilization brings about the experimentally observed increase in frequency.²⁶

(2) An alternative explanation for the observed physical properties of **1** is that inductive and resonance effects are operative. Interactions of this type could bring about sufficient charge delocalization to warrant the assignment of nonintegral oxidation numbers of the two metal atoms. These values would presumably be reflected in the far-ir ligand–metal stretching frequencies of compound **1**. In this interpretation, the shifts to lower frequency in the far-ir are due to decreased electron density at the iron atoms as a result of metal–metal and metal–ligand–metal charge delocalization. This type of interaction could lead to weak bonding between those symmetrical orbitals in **1** whose overlap was sufficiently large. If the doubly degenerate e_{2g} orbitals could interact in this way, two new degenerate molecular orbitals would be formed. The splitting between these four orbitals, β , would result in net stabilization for the molecule when filled with the seven e_{2g} electrons available. Spectral transitions to the upper level of the new e_{2g} orbital would show a hypochromic shift because of the orbital splitting which came about with bond formation.

In addition, as a result of the loss of orbital degeneracy, a new optical transition is expected between the completely filled lower level and the partially filled upper level e_{2g} orbitals. In the limit of small overlap, β will be small and the optical excitation energy of the new absorption band will be low. This interpretation, which allows weak resonance effects, predicts a new, low energy mixed valence band and hypochromic shifts in the far-infrared and visible spectra of compound **1**.

This type of direct interaction alters some details in the double harmonic oscillator diagram of Figure 2. The change in the nature of the electronic states and the increased splitting between the ground state and the excited state as a function of interaction have been discussed by Marcus.²⁸ This means, that in general, $E_{op} \geq 4E_{th}$, where the inequality becomes important when it can be shown there is electron delocalization between the exchanging sites. For biferrocene[Fe(II)Fe(III)] picrate, this means that the calculated thermal electron-transfer rate, $1.3 \times 10^{10} \text{ sec}^{-1}$, may be the lower limit of an exchange process whose physical details depend on the mechanism of intramolecular interaction.

We have discussed two possible interpretations of the mixed valence interaction in compound **1**. These interpretations bear directly on the questions of the origin of the near-infrared spectral transition. One

(24) W. F. Libby, *J. Phys. Chem.*, **56**, 863 (1952).

(25) R. A. Marcus, *J. Chem. Phys.*, **26**, 867 (1957).

(26) Electron-donating properties of the ferrocene substituent in biferrocene have been noted (*cf.* ref 27). In contrast to ferrocene, other electron-donating groups, *i.e.*, CH_3 , cause bathochromic shifts in the ferrocenium transition. These observations can be explained if the inductive effect of ferrocene is due to the molecule's structural similarity to ferrocenium ion or if other mechanisms of interaction are operating.

(27) A. N. Nesmeyanov, S. P. Gubin, E. G. Perovlova, and S. A. Smirnova, *Dokl. Akad. Nauk SSSR*, **147**, 348 (1962).

(28) R. A. Marcus, *Discuss. Faraday Soc.*, **29**, 21 (1960).

possible way in which this question can be resolved is to prepare and study the spectral properties of the biferrocene[Fe(III)Fe(III)] dicationic cation **2**. An electron-transfer transition between two isolated halves of this molecule is unlikely because it would require the formation of a 4+ oxidation state for iron. Barring unforeseen conformational effects, the lack of any absorption in the near-infrared spectral region of **2** would indicate that the band observed in **1** is an electron-transfer band.²⁹ If, on the other hand, there is a transition in the near-infrared spectrum of **2**, this would indicate that the mixed valence band of biferrocene-[Fe(II)Fe(III)] picrate may have arisen from states which were formed from slightly delocalized ferrocene and ferrocenium molecular orbitals.³⁰

Electrical Conductivity. Electrical conductivities (σ) were obtained from the slope of a plot of the measured current through the crystal, I (amperes) vs. applied voltage V . The current values were determined over a large voltage range; the crystal length (L) and area (A) were determined by microscopic measurement.

$$\sigma = IL/VA$$

Compound **1** had a conductivity of $2.3 \times 10^8 \text{ ohm}^{-1} \text{ cm}^{-1}$ at 298°K that was essentially independent of the applied voltage (see Figure 3), over the range of field strengths 10^{-2} V/cm to 10^4 V/cm . If the measured conductivity is due to ionic carriers and not electronic carriers the material should show signs of electrolysis when current flows through the crystal. To test for ionic conduction, a larger amount of charge was passed through the sample than would be allowed by Faraday's law without a drastic change in conductivity. No change could be detected. The conductivity as a function of temperature was found to obey the relationship, $\sigma(T) = \sigma_0 \exp[-E_a/kt]$; that is, the mixed valence organometallic biferrocene salt **1** is a semiconductor at room temperature.

The electrical properties of ferrocene, its charge-transfer complexes, and ferrocenium salts have been studied by several investigators.³¹ Except for the TCNQ⁻ and I₃⁻ salts, in which the conductivity is probably due to the negatively charged anions, almost all the ferrocene compounds are virtual insulators (see Table II). Ferrocene single crystals have been quite extensively studied using a variety of different experimental techniques. The picture that has emerged from these investigations is that the solid consists of localized ferrocene molecules with very weak positive³² charge carrier-lattice coupling.³³ Other high-resistance ferrocene complexes may owe their electrical properties to similar structural features.

(29) In this manner, Taube was able to assign the long-wavelength band of a mixed valence ruthenium compound to an electron-transfer transition (*cf.* ref 20).

(30) Without detailed crystallographic data it is difficult to comment on the feasibility of direct metal-metal interaction of **1**. If structural studies indicate the metal orbitals are not geometrically situated for overlap, then the mixed-valence band could arise from a metal-ligand charge transfer absorption. In the absence of a well understood molecular orbital scheme for ferrocene one cannot make detailed predictions about the electronic structure and spectra of a biferrocene derivative.

(31) F. Gutmann and L. E. Lyons, "Organic Semiconductors," Wiley, New York, N. Y., 1967.

(32) H. Methe and C. Loscoe, *Rev. Sci. Instrum.*, **37**, 1537 (1966).

(33) D. C. Hoesterey and G. M. Letson, *J. Chem. Phys.*, **41**, 675 (1964).

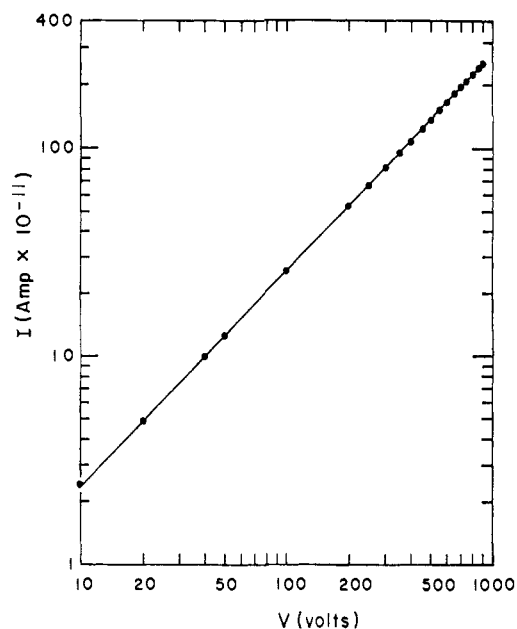


Figure 3. Voltage vs. current graph for a single crystal of biferrocene[Fe(III)Fe(III)] picrate. Only the portion from 10 to 800 V is shown but the curve is linear to at least 10^{-2} V .

The mixed valence transition is also observed in thin-film solid-state spectra of **1** and the relative absorptivities of the thin-film and solution spectra are the same. The band maxima and relative absorptivities probably indicate that very similar geometries and intramolecular interactions are observed in the solid and in solution. Some of the electrical properties of the compound were studied to determine how mixed valence interactions affect bulk transport of charges through a crystal of **1**.

Table II. Conductivity Data

	Log σ , ohm cm ⁻¹	E_a , eV
Ferrocene	10^{-14}	0.89 ^a
Ferrocenium picrate	10^{-13}	
Ferrocene TCNE	10^{-12} ^b	
Ferrocenium ⁺ ₃ ⁻	10^{-9}	0.55 ^c
Biferrocene[Fe(II)Fe(III)] picrate	10^{-8}	0.43
Ferrocenium ⁺ TCNQ ⁻	10^{-1} ^d	

^a E. Zehler and C. Loscoe, "Technical Report 2459," U. S. Army Electronics Research and Development Laboratories, 1964.
^b R. L. Brandon, J. H. Osiecki, and A. Ottenberg, *J. Org. Chem.*, **31**, 1214 (1966).
^c L. R. Melby, *et al.*, *J. Amer. Chem. Soc.*, **84**, 3374 (1962).

The biferrocene[Fe(II)Fe(III)] picrate salt has a room temperature conductivity which is 4-6 orders of magnitude greater than all the ferrocene compounds whose intrinsic conductivity is probably due to the metallocene nucleus. The comparison of **1** and ferrocenium picrate is particularly important inasmuch as both picrates were prepared *via* the same method and subjected to identical purification procedures. In addition, the conductivity measurements were performed in the same manner. One parameter that strongly affects the conductivity is the energy of activation, E_a . These ferrocene compounds have conductivities $\sigma(T)$ which

increase with temperature. The functional relationship they follow is given by

$$\sigma(T) = \sigma_0 \exp(-E_a/kt)$$

From the slope of a plot of σ vs. $1/T$, the activation energy (E_a) for the conduction process was determined. The interpretation of the constant (σ_0) will depend upon the nature of this conduction process involved.³¹ The simplest (but not always correct) interpretation can be obtained by assuming that only one type of carrier is important and that the mobility (μ) is temperature independent. If the number of carriers (n) is determined by a Boltzmann distribution, we can write $\sigma = ne\mu$, $n = N \exp[-E_a/kT]$, $\sigma = Ne\mu \exp[-E_a/kT]$, and $\sigma_0 = Ne\mu$, where N is the total number of available carriers at an (extrapolated) infinite temperature and e is the electronic charge of the carrier. Whereas the assumption may not be true for all these compounds, it is known that ferrocene has one species of charge carrier³² whose mobility is virtually temperature independent.³³

Ferrocene is reported to have a dark conductivity of 10^{-12} – 10^{-14} ohm cm^{-1} and an activation energy from 0.6 to 0.9 eV (see Table II). Using the published value for the mobility of the charge carriers in ferrocene it is possible to calculate N , the maximum number of carriers, for any σ and E_a values. The data for the higher conducting ferrocene crystals ($\sigma = 10^{-12}$, $E_a = 0.6$ eV) leads to an N value of 5×10^{-16} carriers/ cm^3 . Since the usual number of intrinsic carriers expected in organic crystals is of the order of 10^{-21} carriers/ml,³⁴ it seems likely that the lower limit in σ and E_{act} observed in these crystals of Fe is due to an extrinsic impurity controlled conduction process.³⁵ For the more poorly conducting ferrocene ($\sigma = 10^{-14}$ ohm cm^{-1} and $E_a = 0.89$ eV) an N value of 10^{21} can be calculated, which may indicate that these conductivity parameters define the charge-transport process in ferrocene crystals free of electronic impurities. Though the total number of potential carriers in ferrocene is very high, the large activation energy and low measured mobility mean that at room temperature there are relatively few charge carriers moving slowly through the crystal under the influence of the applied field. These factors result in a very small observed true dark conductivity of 10^{-14} ohm cm^{-1} for ferrocene.

The mixed valence ferrocene compound **1**, in striking contrast to ferrocene, was observed to have a room temperature conductivity of 2.3×10^{-8} ohm $^{-1}$ cm^{-1} . This value is 10^6 times that of ferrocene and represents the highest conductivity of any ferrocene compound except for the ferrocene–TCNQ salt. In addition, the conductivity of **1** remained constant over a 10^6 -fold range of field strengths. Though most organic aromatic molecular solids have dark and photoconductivities which cease to be ohmic when the field strength exceeds about 1000 V/cm,³⁴ the biferrocene salt behaved in an ohmic fashion up to 8×10^3 V/cm. This could be due to a high mobility (μ), a large number of carriers (n), or particularly good electrode behavior compared to the other cases studied. Regardless of the cause it

(34) D. R. Kearns, *Advan. Chem. Phys.*, **7**, 282 (1964).

(35) Variations in the measured σ and E_a of ferrocene single crystals have been shown to be due to the number of dislocations in the crystals; cf. ref 31, p 554.

has not been possible to observe the space-charge limited (SCL) region usually found for organic compounds.

Whereas the electrical properties of ferrocene seem to be impurity sensitive, no similar variations in σ or E_a have been observed in crystals of **1**. Calculations of N employing the measured conductivity parameters and reasonable values of μ lead to numbers which indicate that the measured electrical properties of **1** are intrinsic to the material. Even though the total number of available carriers may be the same in ferrocene and compound **1**, the decrease in activation energy of more than 50% means that at a given temperature there are many more free carriers available for charge transport in the mixed valence salt. While we have been able to affect a very large change in activation energy, the mobility of the charge carriers is undoubtedly still very small in **1**. This can be deduced by comparing the activation energy for electronic conduction in **1** (0.43 eV) with the calculated thermal activation energy (0.16 eV) for intramolecular electron transfer. The large difference in these two values can be interpreted to mean that the rate-limiting process is not intramolecular electron transfer but is related to the mechanism by which carriers are transferred between the molecules in the crystal.

The substitution of anions other than picrate may increase intermolecular interaction and carrier mobility. Picrate was originally chosen because it is known³ that ferrocenium picrate has a solid state structure composed of columns of ferrocenium cations and columns of picrate anions. In much the same manner as TCNQ anion radicals are arranged in salts of that compound, the ferrocenium ions in ferrocenium picrate are not separated from each other within any one chain. It was hoped that a similar structural arrangement would prevail in the mixed valence biferrocene salt.

Another way to reduce intermolecular and intramolecular barriers in mixed valence ferrocene salts is to enlarge the size of the ferrocenyl units, thereby decreasing the number of intermolecular barriers seen by the charge carrier. The increase in conductivity with molecular weight and with condensation in aromatic structures is well documented.³⁶ In addition, it has been shown that polyferrocenyl compounds have higher conductivities than ferrocene.³⁷ Therefore, mixed valence ferrocene polymers³³ should show increased electrical conduction over their monomeric analogs. The details of metal–metal interaction in the latter bear quite heavily on the physical characteristics we can ultimately expect in these polymers. A small amount of electron delocalization may lead to partially filled bands resulting in metallic properties for these polymers.

Acknowledgment. The authors acknowledge many helpful discussions on the experimental methods of solid-state physics and chemistry with Drs. Roger Westgate and Jerome Perlstein. Generous support of this work by the Petroleum Research Fund, administered by the American Chemical Society, is acknowledged.

(36) Cf. ref 31, p 450.

(37) H. Watanabe, J. Motoyama, and K. Hata, *Bull. Chem. Soc. Jap.*, **39**, 850 (1966).